

# Extracellular carbonic anhydrase mediates hemorrhagic retinal and cerebral vascular permeability through prekallikrein activation

Ben-Bo Gao<sup>1</sup>, Allen Clermont<sup>1</sup>, Susan Rook<sup>1</sup>, Stephanie J Fonda<sup>1,2</sup>, Vivek J Srinivasan<sup>3</sup>, Maciej Wojtkowski<sup>3</sup>, James G Fujimoto<sup>3</sup>, Robert L Avery<sup>4</sup>, Paul G Arrigg<sup>5</sup>, Sven-Erik Bursell<sup>1,5,6</sup>, Lloyd Paul Aiello<sup>1,5,6</sup> & Edward P Feener<sup>1,2</sup>

**Excessive retinal vascular permeability contributes to the pathogenesis of proliferative diabetic retinopathy and diabetic macular edema, leading causes of vision loss in working-age adults. Using mass spectroscopy-based proteomics, we detected 117 proteins in human vitreous and elevated levels of extracellular carbonic anhydrase-I (CA-I) in vitreous from individuals with diabetic retinopathy, suggesting that retinal hemorrhage and erythrocyte lysis contribute to the diabetic vitreous proteome. Intravitreal injection of CA-I in rats increased retinal vessel leakage and caused intraretinal edema. CA-I-induced alkalinization of vitreous increased kallikrein activity and its generation of factor XIIa, revealing a new pathway for contact system activation. CA-I-induced retinal edema was decreased by complement 1 inhibitor, neutralizing antibody to prekallikrein and bradykinin receptor antagonism. Subdural infusion of CA-I in rats induced cerebral vascular permeability, suggesting that extracellular CA-I could have broad relevance to neurovascular edema. Inhibition of extracellular CA-I and kallikrein-mediated innate inflammation could provide new therapeutic opportunities for the treatment of hemorrhage-induced retinal and cerebral edema.**

The effects of diabetes in the eye are characterized by microvascular abnormalities, proliferation of retinal vessels and increased retinal vascular permeability (RVP), which contributes to nonproliferative diabetic retinopathy (NPDR), proliferative diabetic retinopathy (PDR) and diabetic macular edema (DME), respectively. Among working-age adults in developed countries, PDR and DME are the leading causes of severe and moderate vision loss<sup>1,2</sup>. Although the incidence and progression of diabetic retinopathy can be reduced by intensive glycemic and blood pressure control<sup>3–5</sup>, nearly all people with type 1 diabetes mellitus and over 60% of those with type 2 diabetes mellitus eventually develop this condition. There are over 700,000 people with PDR and 500,000 with macular edema in the United States; an additional 63,000 and 56,000 individuals, respectively, develop these complications each year<sup>2,6</sup>.

Laser photocoagulation is effective for treating the proliferating vessels in PDR and can nearly eliminate blindness from this condition<sup>7</sup>. However, the treatment of DME is much less effective, and therapy for DME remains a major unmet medical need for people with diabetes. DME can occur at any stage of diabetic retinopathy and its incidence increases with the duration of diabetes and the severity

of retinopathy<sup>8</sup>. The condition is characterized by elevated RVP and the loss of retinal endothelial tight-junction integrity, which permits increased diffusion of serum proteins and lipids into the intraretinal space. This can lead to intraretinal fluid retention, lipid deposition and thickening. It becomes sight-threatening when thickening occurs in the macula region<sup>9</sup>, and vision can be transiently or permanently reduced.

Increased RVP occurs shortly after diabetes onset, with the extent of compromise being correlated with the severity of retinopathy<sup>10,11</sup> and the extent of macular thickening<sup>12</sup>. Vascular endothelial growth factor (VEGF) has been considered a principal factor responsible for the increase in RVP in PDR and DME (refs. 13, 14), as well as other conditions such as age-related macular degeneration<sup>15</sup>. Although other vasopermeability factors are clearly involved, our understanding of their relative contributions is incomplete.

Characterization of the vitreous proteome in patients with diabetic retinopathy is likely to provide new insight into the factors and mechanisms responsible for RVP and intraretinal edema, and may improve our understanding of neurovascular edema in other tissues.

<sup>1</sup>Research Division, Joslin Diabetes Center, One Joslin Place, Harvard Medical School, Boston, Massachusetts 02215, USA. <sup>2</sup>Department of Medicine, Harvard Medical School, 25 Shattuck Street Boston, Massachusetts 02115, USA. <sup>3</sup>Department of Electrical Engineering and Computer Science, and Research Laboratory of Electronics, Massachusetts Institute of Technology, 77 Massachusetts Avenue, Cambridge, Massachusetts 02139, USA. <sup>4</sup>Santa Barbara Cottage Hospital Eye Center, 515 E Micheltorena Street, Santa Barbara, California 93103, USA. <sup>5</sup>Beetham Eye Institute, Joslin Diabetes Center, One Joslin Place, Harvard Medical School Boston, Massachusetts 02215, USA. <sup>6</sup>Department of Ophthalmology, Harvard Medical School, 25 Shattuck Street, Boston, Massachusetts 02115, USA. Correspondence should be addressed to E.P.F. (edward.feener@joslin.harvard.edu).

Received 14 July 2006; accepted 13 December 2006; published online 28 January 2007; doi:10.1038/nm1534

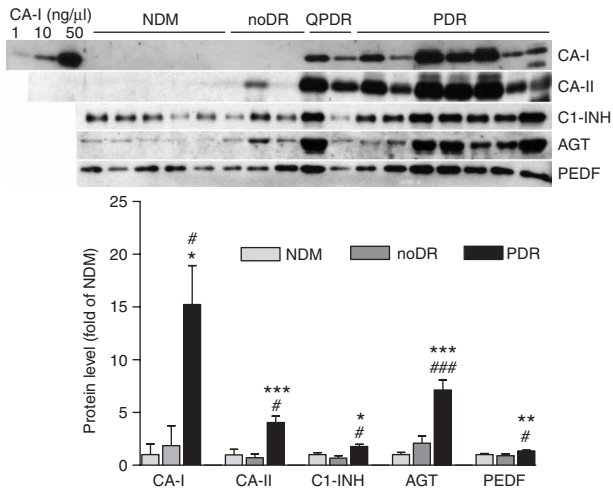


**Figure 1** Western blot analysis of proteins from vitreous samples. Top, representative western blot showing immunoreactivity of proteins in NDM, noDR, quiescent PDR (QPDR) and PDR subjects. The immunoreactivity of antibody to CA-I is shown with purified CA-I standards. Bottom, bar graph quantitation of western blot results for the proteins indicated in the three groups of samples (mean  $\pm$  s.e.m.  $n = 3-10$ ). \* $P < 0.05$ , \*\* $P < 0.01$ , \*\*\* $P < 0.001$  versus NDM; # $P < 0.05$ , ### $P < 0.001$  versus noDR.

## RESULTS

### Comparison of nondiabetic and diabetic vitreous proteomes

We obtained undiluted vitreous samples at the time of pars plana vitrectomy from 25 subjects. Individuals were nondiabetic (NDM,  $n = 8$ ), diabetic with no diabetic retinopathy (noDR,  $n = 4$ ) or diabetic with PDR ( $n = 13$ ). The demographics are summarized in **Supplementary Table 1** online.

We performed proteomic analysis on randomly selected vitreous from NDM ( $n = 5$ ), noDR ( $n = 4$ ) and PDR ( $n = 3$ ) individuals. Vitreous samples were separated by SDS-PAGE and the protein inventories of each sample were identified using tandem mass spectroscopy. We compiled the proteins identified from the vitreous samples and assessed the numbers of unique peptides for each protein and subject (**Supplementary Table 2** online). We identified 117 proteins in the vitreous, ranging in size from 10 kDa to 500 kDa; these included 64, 113 and 107 proteins in the NDM, noDR and PDR samples, respectively. Immunoglobulin components were present in all samples and are not listed. We evaluated protein differences among the three groups by the absence or presence of protein detection and by differences in the extent of peptide coverage. Kruskal-Wallis analysis of ranks based on the numbers of unique peptides indicated that 31 proteins were differentially detected among the three groups, including transport proteins (afamin, apolipoprotein A-I, apolipoprotein A-IV, apolipoprotein B-100, apolipoprotein C-III and apolipoprotein D); acute-phase response proteins ( $\alpha$ -1-antitrypsin,  $\alpha$ -2-HS-glycoprotein, angiotensinogen (AGT), chitinase 3-like 1, orosomucoid-1 and orosomucoid-2); proteins involved in cell growth, maintenance and metabolism (carbonic anhydrase I (CA-I), GAPDH, gelsolin isoform a and pigmented epithelium-derived factor (PEDF)); complement system proteins (complement C4B, complement component 9 and clusterin isoform 1); and cell adhesion proteins ( $\alpha$ -2-glycoprotein 1-zinc and galectin-3 binding protein). Compared with the NDM samples, there were 27, 18 and 31 proteins whose levels were elevated in the PDR, noDR and PDR + noDR groups, respectively.

Validation of protein changes by western blot analysis revealed that CA-I concentration in the vitreous of the PDR group ( $n = 8$ ) was 15.3 ( $P < 0.01$ ) and 8.2 ( $P < 0.05$ ) times higher than that in the NDM ( $n = 6$ ) and noDR ( $n = 4$ ) groups, respectively (**Fig. 1**). We detected substantial levels of CA-I in the vitreous from people with quiescent proliferative diabetic retinopathy (QPDR), who have undergone laser photocoagulation therapy and do not have active new vessel proliferation (**Fig. 1**). The two QPDR results shown are representative of a total

of 9 QPDR samples that were examined. Also, compared to NDM subjects, CA-I levels were 15 times higher in individuals with moderate or severe NPDR ( $n = 5$ ) characterized by microvascular lesions including microaneurysms and retinal hemorrhage but no signs of proliferative retinopathy (data not shown). In PDR vitreous, CA-II was elevated 4-fold ( $P < 0.001$ ) and 5.6-fold ( $P < 0.05$ ), respectively, compared to that in noDR and NDM vitreous. In addition, PDR vitreous had increased concentrations of complement 1 inhibitor (C1-INH, 1.8-fold), AGT (7.1-fold) and PEDF (1.4-fold) compared with the NDM group (**Fig. 1**).

### Carbonic anhydrase induces retinal vascular permeability

A notable finding was the identification of the intracellular enzyme CA-I in the PDR vitreous proteome. At least 12 active isoforms of CA catalyze the hydration of carbon dioxide to bicarbonate. Certain functions of cell-associated CA isoforms are well documented<sup>16,17</sup>, but the physiological effects of soluble extracellular CA in the vitreous fluid are unknown. Although a molecular connection between increased CA levels and diabetic retinopathy has not been previously identified, a pilot study has suggested that the CA inhibitor acetazolamide may have beneficial effects in individuals with DME, as assessed by fluorescein-angiographic and perimetric data (ref. 18).

Comparison with purified CA-I standards demonstrated that the concentration of CA-I in the PDR vitreous ranged from 10–50 ng/ $\mu$ l (**Fig. 1**). Injection of purified human CA-I into the rat vitreous (to reach a concentration of 2 ng/ $\mu$ l) induced retinal fluorescein leakage 30 min later, as compared to baseline levels or to eyes that received a control intravitreal injection of balanced saline solution (BSS, **Fig. 2a**). CA-I-induced RVP was inhibited by co-injection of 1  $\mu$ M acetazolamide, indicating that CA-I enzymatic activity was necessary for its effect on RVP. At 48 h after intravitreal CA-I injection, we observed focal areas of retinal vascular leakage using both fluorescein (**Fig. 2b**) and 2,000 kDa fluorescein-dextran conjugate (**Fig. 2c**).

Although increased RVP can occur within 1 week of diabetes onset<sup>19</sup>, early diabetes alone is usually not sufficient to induce intraretinal thickening because the eye has numerous mechanisms to equilibrate retinal fluid balance. Furthermore, animal models of diabetes generally do not result in actual retinal thickening, even though increased RVP is evident. We postulated that the combined effect of diabetes and intravitreal CA-I on the retina might exceed the counter-regulatory mechanisms involved in ocular fluid balance and lead to retinal thickening. As we found focal areas of leakage using fluorescein-dextran at 48 h after intravitreal injection (**Fig. 2b,c**), we used this time point to investigate the effect of intravitreal injection of CA-I on retinal ultrastructure, using high-speed, ultrahigh resolution optical coherence tomography (OCT)<sup>20</sup>. Using OCT imaging with 2.8- $\mu$ m axial image resolution to visualize and measure retinal morphology, we observed that at 48 h after intravitreal injection, the retinas of diabetic rats receiving CA-I were 12% thicker and the outer nuclear layer (ONL) 30% thicker than in contralateral eyes receiving an intravitreal saline vehicle injection (**Fig. 2d**). Indeed, in CA-I-treated eyes, the ONL accounted for 38% of the overall retinal

thickness, an increase of 17% and 18%, respectively, compared to BSS-treated diabetic and nondiabetic rats. These data provide the first evidence, to our knowledge, of an endogenous molecule that induces clinically evident intraretinal edema in the diabetic rat model at physiologically relevant concentrations.

Intravitreal injection of CA-I increased RVP, as measured by vitreous fluorophotometry, in a dose-dependent manner (Fig. 3a): the maximal stimulation was 2.3 times the baseline value ( $P < 0.001$ ) at 20 ng/ $\mu$ l in the vitreous. The vitreous concentration of CA-I that induced its half maximal effect on RVP was 0.67 ng/ $\mu$ l. Intravitreal injection of CA-II (to reach a concentration of 2 ng/ $\mu$ l) increased RVP by 2.4 times compared to baseline. The effect of a single dose of CA-I on RVP was sustained at 24 h after injection at a level 59% higher than that in the control (Fig. 3b). Intravitreal injection of human serum albumin (HSA) to reach a concentration of 2 ng/ $\mu$ l or heat-inactivated CA-I (96 °C, 5 min) did not affect RVP (Fig. 3c), showing that permeability was not the result of introducing a human protein into the rat vitreous. CA-I-induced RVP was inhibited 68% and 90%, respectively, by co-injection of 1  $\mu$ M acetazolamide or 0.5  $\mu$ M methazolamide ( $P < 0.001$ ); these sulfonamide CA inhibitors did not affect basal RVP.

RVP was higher in rat eyes receiving an intravitreal injection of 10  $\mu$ l vitreous from PDR individuals than in rat eyes receiving similar injections from no-PDR individuals (noDR and NDM,  $P = 0.02$ ) or in those receiving the BSS control ( $P < 0.05$ , Fig. 3d). The effect of vitreous from noDR and NDM groups was not substantially different from that of the BSS control. To determine the contribution of CA activity to PDR vitreous-induced RVP, vitreous from the human subjects was pretreated with 10  $\mu$ M acetazolamide or BSS control before transfer into rat vitreous. Acetazolamide reduced RVP in rat eyes injected with vitreous from PDR subjects to a level comparable to that in rat eyes injected with vitreous from no-PDR subjects (Fig. 3d).

The appearance of CA-I in the vitreous correlated with the presence of 14 other proteins, including plasma proteins ( $\alpha$ 2-plasmin inhibitor; apolipoproteins A-II, B-100 and C-III; complement C9 and factor H; fibrinogen  $\gamma$ -chain; kininogen; and leucine-rich  $\alpha$ 2-glycoprotein 1)<sup>21</sup> and cytoplasmic erythrocyte proteins (biliverdin reductase B; and hemoglobin  $\alpha$ -chain,  $\beta$ -chain and  $\delta$ -chain) (Supplementary Table 2). As both CA-I and CA-II are cytoplasmic proteins expressed in erythrocytes and ocular tissues<sup>22</sup>, the increased appearance of these isoforms in the PDR vitreous could be the result of local tissue injury or lysed red blood cells (RBC) from intraocular hemorrhage.

To test whether CA derived from lysed RBC could induce RVP, we injected lysed RBC into the vitreous of rats. Intravitreal injection of lysed RBC or CA-I into rats increased RVP 4.1-fold and 3.0-fold, respectively, compared with that in eyes receiving a BSS injection (Fig. 3e). Pretreatment of lysed RBC with acetazolamide (10  $\mu$ M) blocked the increase in RVP. These results suggest that the release of CA-I into the vitreous from an intraocular hemorrhage could increase RVP.

### Mechanisms mediating carbonic anhydrase-induced RVP

Intravitreal injection of CA-I to reach a concentration of 2 ng/ $\mu$ l increased RVP 2.4-fold compared with that in BSS-injected eyes ( $P < 0.001$ ) (Fig. 3f). The magnitude of this effect was slightly greater than that observed with intravitreal injection of VEGF (to reach a concentration of 0.02 ng/ $\mu$ l), and the two responses were additive. Co-injection of C1-INH, a serpin protease inhibitor of classical complement activation and the kallikrein system, inhibited CA-I-stimulated RVP by 92%. C1-INH had no effect on basal or VEGF-induced RVP. Co-injection of other serpin family proteins, including PEDF and angiotensinogen, did not inhibit CA-I-induced RVP (data not shown).

Although the role of C1-INH in angioedema is well documented<sup>23</sup>, its role in retinal edema has not been previously described. C1-INH

deficiency increases vascular permeability in the skin through increased generation of bradykinin (BK) generation and the BK2 receptor pathway<sup>24</sup>. We further examined the role of the kallikrein-kinin pathway in CA-I-induced RVP. Co-injection of the respective BK2 and BK1 receptor antagonists Hoe 140 or [des-Arg<sup>10</sup>]-Hoe140 (to reach an intravitreal concentration of 1  $\mu$ M) reduced CA-I's induction of RVP by 67% and 45%, respectively (Fig. 3g). Treatment with both BK antagonists blocked CA-I's induction of RVP by 78% ( $P < 0.001$ ). The carboxypeptidase inhibitors leupeptin and aprotinin block proteolytic activation of kallikrein<sup>25,26</sup>. Intravitreal injection of either leupeptin or aprotinin (to reach a concentration of 10  $\mu$ M) ameliorated CA-I-induced RVP by 71% and 50%, respectively, without altering basal leakage (Fig. 3f). Co-injection of antibody to prekallikrein (anti-PK), which sterically blocks its activation by FXIIa (ref. 27), blocked CA-I-stimulated RVP by 81% (Fig. 3h). In contrast, anti-PK antibody pretreatment did not affect RVP stimulated by intravitreal injection of VEGF (Fig. 3h). We monitored the effects of C1-INH and anti-PK on the kinetics of PK activation by factor XII (FXII) *in vitro* using a fluorescent kallikrein

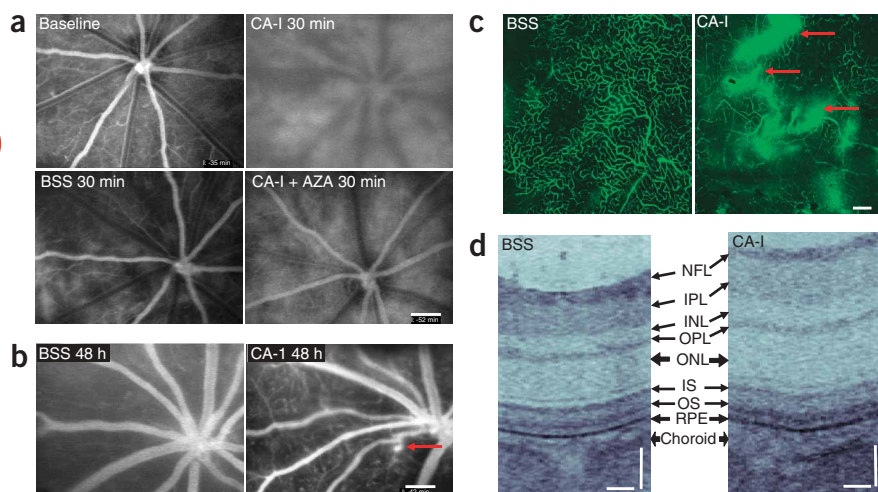


**Figure 2** Intravitreal CA-I induces retinal vascular permeability. (a) Fluorescein angiography of rat retina at baseline and 30 min after intravitreal injection of BSS vehicle, CA-I or CA-I + acetazolamide (AZA). Scale bar, 200  $\mu$ m. (b) Fluorescein angiography 48 h after intravitreal injection with BSS or CA-I. Scale bar, 200  $\mu$ m. (c) Confocal (10 $\times$ ) fluorescence microscopy of retinal flatmounts 48 h after intravitreal injection of BSS or CA-I. Scale bar, 50  $\mu$ m. For (b) and (c), focal areas of fluorescein leakage and accumulation are indicated with red arrows. (d) Retinal edema in a rat receiving intravitreal CA-I. Fourier domain high-speed ultrahigh-resolution optical coherence tomography of diabetic rat retina 48 h after intravitreal injection of saline or CA-I (to reach a concentration of 2 ng/ $\mu$ l). Retinal layers labeled are nerve fiber layer (NFL), inner plexiform layer (IPL), inner nuclear layer (INL), outer plexiform layer (OPL), outer nuclear layer (ONL), inner segment (IS), outer segment (OS) and retinal pigment epithelium (RPE). Scale bar, 50  $\mu$ m. In a–d, representative results from three experiments are shown.

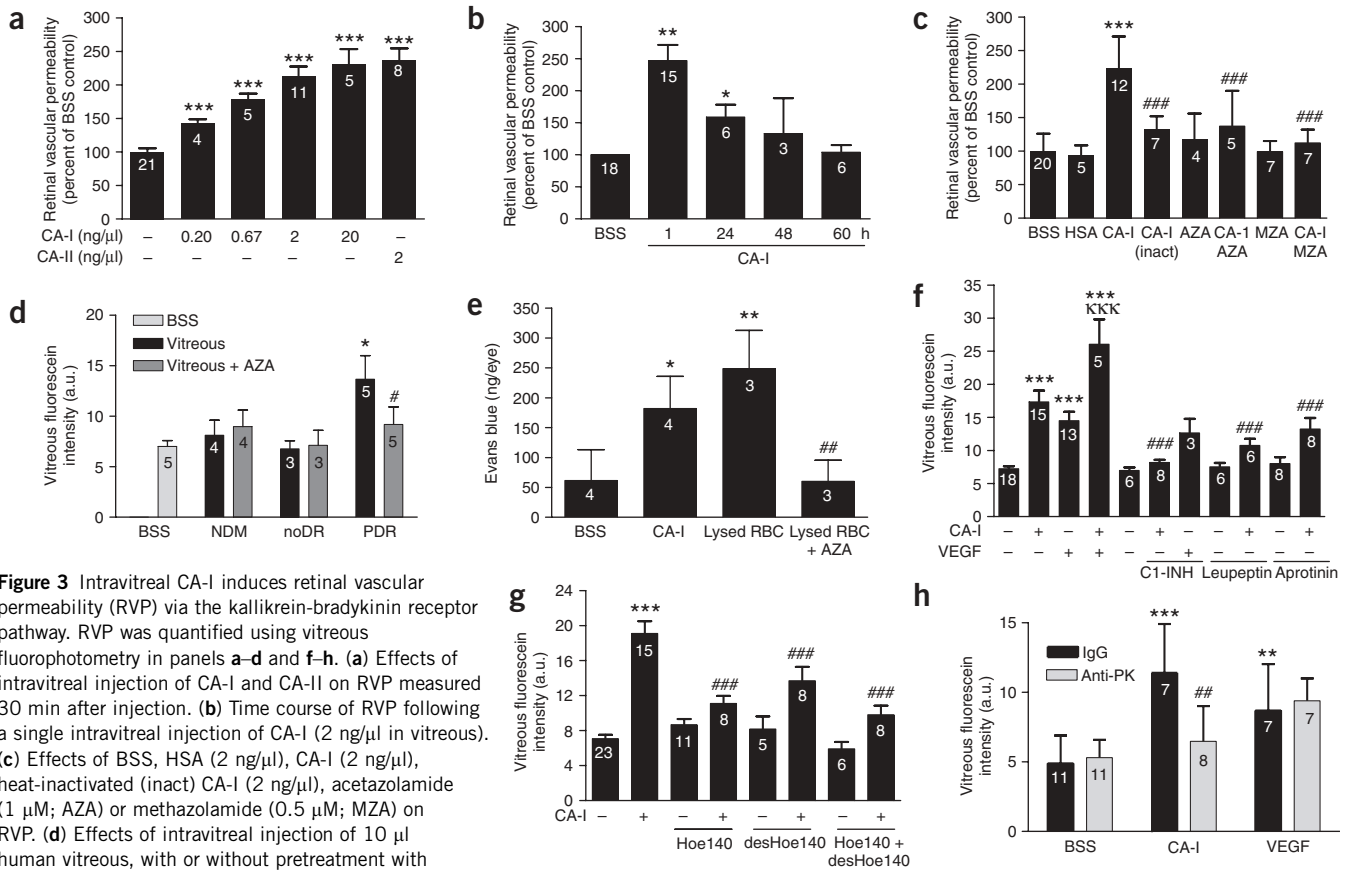


**Figure 3** Intravitreal CA-I induces retinal vascular permeability (RVP) via the kallikrein-bradykinin receptor pathway. RVP was quantified using vitreous fluorophotometry in panels **a–d** and **f–h**. **(a)** Effects of intravitreal injection of CA-I and CA-II on RVP measured 30 min after injection. **(b)** Time course of RVP following a single intravitreal injection of CA-I (2 ng/μl in vitreous). **(c)** Effects of BSS, HSA (2 ng/μl), CA-I (2 ng/μl), heat-inactivated (inact) CA-I (2 ng/μl), acetazolamide (1 μM; AZA) or methazolamide (0.5 μM; MZA) on RVP. **(d)** Effects of intravitreal injection of 10 μl human vitreous, with or without pretreatment with acetazolamide, on RVP. **(e)** Effects of CA-I and lysed RBC on RVP using Evans blue dye. **(f)** Effects of CA-I (2 ng/μl), VEGF (0.02 ng/μl), C1-INH (2 ng/μl), leupeptin (10 μM) or aprotinin (10 μM) on vitreous fluorescein intensity. **(g)** Inhibition of CA-I-induced vitreous fluorescein leakage by Hoe140 (1 μM) or [des-Arg<sup>10</sup>]-Hoe140 (1 μM; desHoe140). **(h)** Effects of intravitreal injection of antibody to prekallikrein (anti-PK, 33 ng/μl) and normal mouse IgG (33 ng/μl) on CA-I- and VEGF-stimulated RVP. Data represent mean ± s.d. \**P* < 0.05, \*\**P* < 0.01 and \*\*\**P* < 0.001 versus BSS. #*P* < 0.05 versus untreated PDR vitreous (**d**), ##*P* < 0.01 versus lysed RBC (**e**) or IgG + CA-I (**h**), ###*P* < 0.001 versus CA-I, KKK*P* < 0.001 versus VEGF (**f**). a.u., arbitrary units. Numbers in bars indicate animals per group.

substrate. These experiments confirmed that PK activation was inhibited by C1-INH and anti-PK (**Supplementary Figs. 1 and 2** online). As bradykinin can induce permeability via activation of nitric oxide synthase (NOS), we investigated the effect of NOS inhibition on CA-I-induced permeability. Intravitreal injection with nitro-*L*-arginine methyl ester (10 μM) inhibited CA-I-induced RVP by 62% (*P* < 0.05, data not shown).

CA plays a central role in the regulation of extracellular pH, and the retina contains robust mechanisms for ion transport<sup>28</sup>. We measured the effect of CA-I on vitreous pH by using a microminiature electrode via an opening through the sclera and with a pH-sensitive fluorescent probe (2',7'-bis-(2-carboxyethyl)-5-(and-6)-carboxyfluorescein (BCECF) conjugated to 70 kDa dextran). Using the electrode, we found that the pH of vitreous 5 min after injection of CA-I was 7.8 ± 0.21, compared with a pH of 7.4 ± 0.15 following injection of BSS vehicle (*P* < 0.002) (**Fig. 4a**). We also used this electrode to directly measure the pH of vitreous following an intravitreal injection with BCECF-dextran dye in either BSS (pH 7.4) or HEPES buffer (pH 8.0) following measurement of vitreous fluorescence. Using this minimally invasive pH-sensitive dye and the reference pH measured using the electrode, we calculated the vitreous pH to be 7.96 ± 0.38 following intravitreal injection of CA-I. To determine the effect of an alkaline pH on RVP, BSS with a pH adjusted to 7.4 or 8.0 was injected into the

vitreous, and retinal fluorescein leakage was monitored by fluorescein angiography. Intravitreal injection of BSS at pH 7.4 did not produce a detectable effect on vascular leakage (**Fig. 4b**). In contrast, intravitreal injection of BSS at pH 8.0 increased RVP to an extent comparable to that observed following CA-I injection. Intravitreal injection of the neutralizing anti-PK antibody reduced the increase in RVP induced by subsequent injection of BSS of pH 8.0 (**Fig. 4b**).

As our data showed that anti-PK antibody blocked RVP induced by both CA-I and BSS of pH 8.0 (**Figs. 3h and 4b**), we looked for the presence of components of the kallikrein system in human vitreous and investigated the effect of pH on the kallikrein pathway. Activation of the kallikrein system via the contact system involves both kallikrein-mediated cleavage of FXII to FXIIa and FXIIa-mediated cleavage of PK to kallikrein. We found that vitreous from individuals with PDR contained PK, kallikrein, FXII, FXIIa and kininogen heavy chain (**Fig. 4c**). Based on a comparison to 20 ng of purified PK or FXII, we found that PDR vitreous contained low μg/ml levels of these proteins. We also detected high molecular weight kininogen (HK) in our proteomic analysis (**Supplementary Table 2**). The appearance of both kallikrein and FXIIa in these samples suggested that the contact system is present and activated in the vitreous of individuals with PDR.

We monitored the effect of pH on the kinetics of PK activation in the presence of FXII *in vitro* using a fluorescent kallikrein substrate.

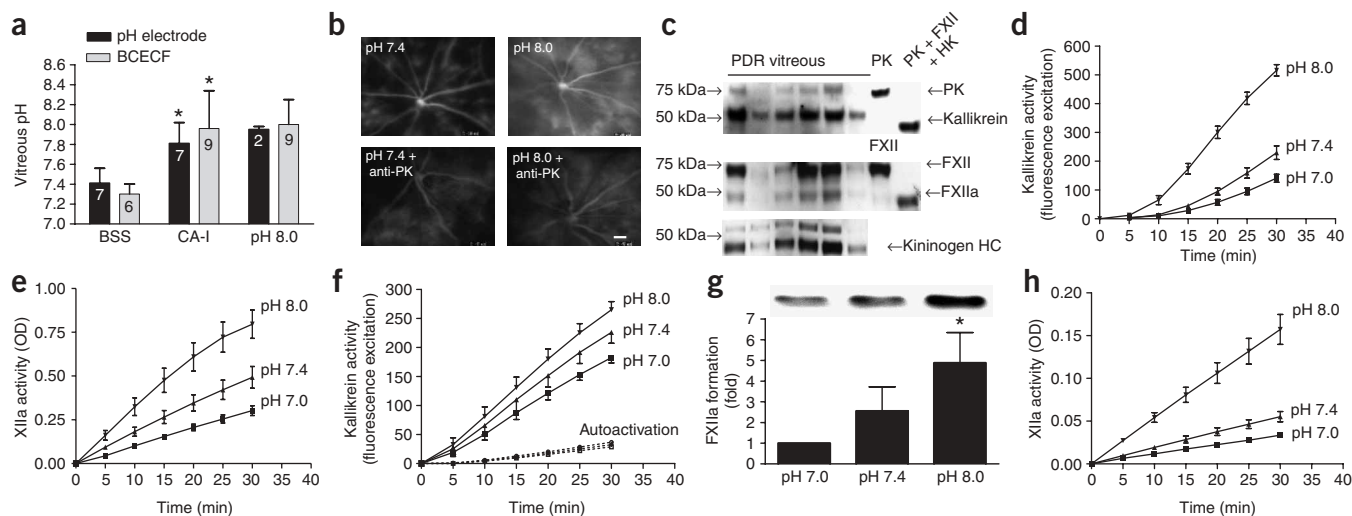


**Figure 4** Effect of CA-I on vitreous pH and effects of pH on RVP and activity of the components of the kallikrein system. **(a)** Effects of CA-I on vitreous pH measured by microelectrode and fluorescent indicator (BCECF). \* $P < 0.05$  versus BSS. Data represent mean  $\pm$  s.d. **(b)** Effects of intravitreal injections of BSS pH 7.4 and BSS pH 8.0 on RVP. RVP was visualized using fluorescein angiography, as shown in **Figure 2**. Representative images from at least three independent experiments are shown. Scale bar, 200  $\mu$ m. **(c)** Western blot analysis of PK/kallikrein, FXII/FXIIa and kininogen heavy chain (HC) in vitreous (vitreous loaded on the gel: 4  $\mu$ l, 1  $\mu$ l and 0.25  $\mu$ l, respectively) from six individuals with PDR. Purified standards of PK or FXII (20 ng) alone and the reaction mixture generated from a 1-h-long, room temperature 24 °C incubation of PK, FXII and HK to generate kallikrein and FXIIa are shown in lanes on the right. **(d)** Effects of pH on PK activation in the presence of FXII and HK. **(e)** Effects of pH on FXII activation in the presence of PK and HK. **(f)** Effects of pH on kallikrein activity (solid lines) and PK autoactivation (dashed lines) in the absence of FXII and HK. **(g)** Effects of pH on FXIIa formation from FXII by kallikrein in the presence of HK and kaolin. Western blot of FXIIa and bar graph quantitation of FXIIa generation are shown. \* $P < 0.05$  versus pH 7.4. **(h)** Effects of pH on FXII activation by kallikrein in the presence of HK and kaolin. In **d-h**, data represent mean  $\pm$  s.e.m. of at least three independent experiments. OD, optical density.

The kinetics of PK activation in the presence of FXII and HK was facilitated by alkaline pH compared to neutral pH (**Fig. 4d**). Neither CA-I or bicarbonate ion affected PK activation *in vitro* (**Supplementary Fig. 3** online). Moreover, the increase in PK activation by alkaline pH required the combination of FXII, PK and HK (**Supplementary Fig. 4** online). Alkaline pH increased FXII activation in the presence of PK and kaolin (**Fig. 4e**) but did not affect FXII autoactivation in the absence of PK (**Supplementary Fig. 5** online). In contrast, kallikrein activity in the absence of FXII was increased at a pH of 8.0 compared with a pH of 7.4, but alkaline pH did not affect PK autoactivation (**Fig. 4f**). Moreover, both kallikrein-mediated generation of FXIIa protein and FXIIa activity were enhanced by alkaline pH (**Fig. 4g,h**). These results show that the pH-sensitive event in kallikrein activation is the increase in kallikrein activity, which augments the generation of the PK activator FXIIa.

### Carbonic anhydrase increases cerebral vessel permeability

To investigate whether extracellular CA could have broad relevance to vasogenic edema, we investigated the effect of CA-I on blood-brain barrier permeability. Previous reports have shown that one or more factors released from lysed RBC induce edema following intracerebral

hemorrhage<sup>29</sup>. Indeed, factors released from the hematoma to the brain parenchyma have been implicated in the delayed onset of cerebral edema and secondary neuronal injury in the days following

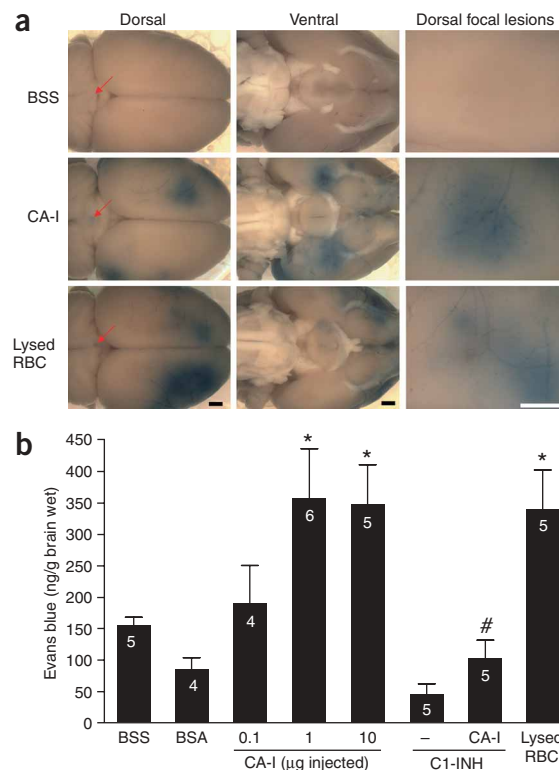


**Figure 5** CA-I increases blood-brain barrier permeability to Evans blue dye. **(a)** Photograph of the dorsal and ventral surfaces, and 3 $\times$  magnification of dorsal focal lesions of the rat brain 24 h after subdural space injection (indicated by arrows) of 50  $\mu$ l BSS vehicle, 1  $\mu$ g/50  $\mu$ l CA-I and 12.5  $\mu$ l lysed RBC per 50  $\mu$ l BSS. Scale bars, 0.1 cm. **(b)** Evans blue was extracted and quantified from the brain surface 24 h after subdural space injection of 50  $\mu$ l BSS vehicle, 1  $\mu$ g/50  $\mu$ l CA-I or 10  $\mu$ g/50  $\mu$ l BSA or C1-INH. Data represent mean  $\pm$  s.e.m.  $n = 4-6$  rats. \* $P < 0.05$  versus BSS. # $P < 0.05$  versus 1  $\mu$ g CA-I.

an intracerebral hemorrhage<sup>30</sup>. Using a rat model to assess blood-brain barrier permeability, we found that infusion of CA-I or lysed RBC into the subdural space induced intense focal areas of Evans blue leakage on the dorsal and ventral surfaces of the brain (Fig. 5a); this was not observed in rats that received an infusion with BSS vehicle. CA-I-induced cerebral vascular permeability occurred in areas distal to the infusion site, consistent with diffusion of CA-I in the cerebral fluid. Quantification of Evans blue dye showed that CA-I and lysed RBC increased permeability in the brain 2.3-fold and 2.2-fold, respectively, compared to that in rats that received BSS ( $P < 0.05$ , Fig. 5b). In contrast, rats that received C1-INH or albumin had similar or slightly lower levels of permeability compared with rats that received the BSS control. C1-INH blocked CA-I-induced cerebral vascular permeability in a manner similar to that seen for RVP (Fig. 3f). These results suggest that the release of CA-I from lysed RBC following cerebral hemorrhage could contribute to increased blood-brain barrier permeability and edema.

## DISCUSSION

Using mass spectroscopy-based proteomics, we have characterized the vitreous proteome from nondiabetic people and from diabetic people either without diabetic retinopathy or with PDR. We identified 117 proteins from human vitreous, compared with the 20–50 proteins previously described in vitreous using two-dimensional gel electrophoresis<sup>31–33</sup>. Our experimental approach was to use preparative one-dimensional SDS-PAGE to examine independently the vitreous proteome from 12 individuals rather than a representative sample. This approach probably contributed to the higher number of proteins identified compared with previous studies.

The appearance of CA-I and CA-II in the vitreous correlated with other cytoplasmic erythrocyte proteins, suggesting that ocular hemorrhage contributed to the appearance of CA in the vitreous fluid from individuals with PDR. As CA was not detected in the vitreous from nondiabetic subjects, it is likely that its appearance in the PDR vitreous was derived from pathologic ocular hemolysis rather than surgically induced blood contamination during pars plana vitrectomy. PDR individuals often have nascent preretinal vessels that are a source of pathological hemorrhage. We also detected CA-I in vitreous from individuals with moderate or severe NPDR, who do not have retinal neovascularization, suggesting that CA-I in the vitreous might also be derived from intraretinal hemorrhage.

Although idiopathic vitreous hemorrhage in the absence of retinal pathology is not a recognized cause of retinal swelling, the clinical effects of hemorrhage on RVP have not been reported. Retinal and vitreous hemorrhages are commonly associated with moderate to severe NPDR or PDR. In addition, diabetes itself is associated with increased RVP. Therefore, the ability of the retina to compensate for an additional increase in RVP due to retinal hemorrhage could be compromised in diabetes, resulting in the accumulation of intraretinal fluid.

It is well established that DME becomes more prevalent as the severity of retinopathy increases. One of the criteria used to assess NPDR severity is the extent of intraretinal hemorrhage—which, when prominent, can lead to a diagnosis of severe NPDR, even if it is the only abnormality present in all retinal quadrants. DME risk can increase four-fold from mild to severe NPDR (ref. 34). In addition, DME commonly occurs with PDR in cases where vitreous hemorrhage and/or severe retinal hemorrhage are present. If intraocular hemorrhage induces edema only in specific areas of the diseased retina, this might account for the observation that edema can occur at a location distant from the site of hemorrhage.

The magnitude of CA-I's effect on RVP was equivalent to that of the potent permeability factor VEGF. Acetazolamide blocked the permeability effect of human PDR vitreous when injected into the rat eye, indicating that CA activity accounts for a substantial portion of the effects of injected vitreous on retinal permeability in PDR. Our results suggest that the release of CA-I to the vitreous following a retinal or vitreous hemorrhage could play an important role in the high levels of RVP and retinal edema that occur in PDR. Moreover, as retinal ischemia is associated with diabetic retinopathy, it is possible that extracellular CA could hydrate carbon dioxide during hypoxia and act additively with VEGF to increase retinal permeability<sup>35</sup>. Indeed, the effect of CA-I on RVP was additive with VEGF's effect.

We showed that inhibitors of kallikrein activation, including a neutralizing anti-PK antibody, C1-INH and carboxypeptidase inhibitors<sup>24</sup>, blocked CA-I-induced RVP as did inhibitors of the bradykinin receptors BK1 and BK2. These findings demonstrate that the kallikrein-kinin pathway mediates the vascular permeability effects induced by extracellular CA. We showed that introduction of CA-I into the vitreous increased vitreous pH and that alkaline pH increased kallikrein activity and kallikrein-mediated activation of FXII, suggesting a new mechanism for kallikrein-kinin activation. However, the contact activation system is complex and multifactorial, and thus the sequence of events and regulatory components involved in PK activation are likely to be tissue and body fluid specific.

A recent report has shown that targeted disruption of the gene encoding FXII reduces basal plasma bradykinin levels by 50% and completely blocks contact-stimulated bradykinin production<sup>36</sup>. These results suggest that both FXII-dependent and FXII-independent pathways of PK activation contribute to basal plasma kallikrein activity. An FXII-independent mechanism of PK activation involves prolyl-carboxypeptidase, which is constitutively expressed on the plasma membrane of endothelial cells<sup>37</sup>. The optimum pH for prolyl-carboxypeptidase-mediated PK activation is 7.1 (ref. 25), whereas we report that PK activation in the presence of FXII was increased at pH 8.0 compared with pH 7.0 and 7.4 (Fig. 4d). Although both FXII-dependent and FXII-independent mechanisms may contribute to ocular PK activation, our results suggest that CA-I-induced alkalization of vitreous can activate basal kallikrein activity, which would facilitate the kallikrein-mediated positive-feedback pathway via FXII activation (Fig. 4g,h and ref. 38).

CA isoenzymes differ in their tissue distribution, subcellular localization and their susceptibility to CA inhibitors, measured as the inhibitor concentration required to produce half maximum inhibition ( $K_i$ ). Multiple CA isozymes are expressed in the retina, including membrane-associated CA-IV and CA-XIV, which have been implicated in facilitating the removal of CO<sub>2</sub> from the neuroretina and in photoreceptor function<sup>28,39</sup>. Systemic CA inhibition using acetazolamide increases retinal and cerebral blood flow, oxygen concentration in the optic nerve and blood CO<sub>2</sub> levels<sup>40–42</sup>. Effects of CA inhibitors on glaucoma and macular edema have been previously attributed to the inhibition of CA-II and CA-IV and bicarbonate-coupled active ion transport<sup>16,17</sup>. We showed that both CA-I and CA-II are elevated in vitreous of individuals with diabetic retinopathy, which may lead to the accumulation of bicarbonate inside the blood retinal barrier. Although CA-II and CA-IV are inhibited by acetazolamide and dorzolamide at low (nM) concentrations, the  $K_i$  of these inhibitors is 250 nM and 50 μM, respectively, for CA-I (ref. 43). As the  $K_i$  of CA inhibitors for CA-I can range over 2 or 3 orders of magnitude, isoenzyme-selective inhibitors may provide opportunities to target specific retinal functions and pathologies. Our findings also suggest that proteins downstream of CA-I, including C1-INH and antagonists

of the kallikrein system, could also represent therapeutic targets for inhibiting CA-I-induced vascular permeability. Recombinant C1-INH is currently being investigated as a treatment for hereditary angioedema<sup>44</sup>. Our results suggest that C1-INH or other kallikrein inhibitors warrant further investigation as treatments for RVP in advanced diabetic retinopathy. However, as bradykinin B2 receptor deficiency increases albuminuria and glomerular mesangial sclerosis in *Ins2<sup>Akita</sup>* mice<sup>45</sup>, it is possible that complete systemic blockade of BK2 receptor action could have adverse vascular effects.

In summary, our data show that the presence of extracellular CA-I inside either the blood-retinal or blood-brain barrier can induce vasogenic edema. The release of erythrocyte CA-I may account for the increased vascular permeability and edema in diabetic retinopathy or following subdural hematoma. Thus, delivery of extracellular CA-I-selective inhibitors, C1-INH or antagonists of the kallikrein-kinin system may provide new opportunities for the treatment of neurovascular edema associated with conditions such as PDR, DME, age-related macular degeneration and cerebral hemorrhage.

## METHODS

**Study subjects and sample collection.** Vitreous fluid was obtained from individuals undergoing pars plana vitrectomy at the Beth Israel Deaconess Medical Center and the Santa Barbara Cottage Hospital Eye Center, in accordance with Human Discarded Specimen Research Protocol approved by institutional review boards at both institutions. Undiluted samples were collected at the time of surgery, immediately placed on ice, spun at 15,000g for 1 min to remove insoluble material and stored at  $-80^{\circ}\text{C}$  until used.

**Proteomic analysis.** Proteomic analysis was performed on 50  $\mu\text{l}$  of vitreous from NDM subjects, noDR individuals and PDR individuals. The absence of diabetic retinopathy or presence of PDR was defined as level 10 or  $>60$ , respectively, on the Early Treatment Diabetic Retinopathy Study (ETDRS) grading scale<sup>46</sup>. Soluble proteins were separated by 12% SDS-PAGE, and the entire lane for each sample was divided into slices of 1 mm width. In gel, tryptic digests from the entire lane were analyzed by tandem mass spectrometry (MS/MS) using an LTQ linear ion trap mass spectrometer (Thermo Electron). Assignment of MS/MS data was performed using SEQUEST software (Thermo Electron). Resultant matches were entered and compiled into a MySQL database, and proteomics computational analyses were performed using a Hypertext Preprocessor (PHP)-based program. First, peptide identifications were made based on the following criteria: cross-correlation score  $> 1.5$ , 2.0 and 2.5 for charge states +1, +2 and +3, respectively; delta correlation  $> 0.1$ ; primary score  $> 200$ ; ranking of the primary score  $< 3$ ; and percent fragment ions  $> 30\%$ . Second, protein identifications were assigned when the following criteria were met: the unique peptide match number was greater than or equal to two, peptides contributing to protein matches were derived from a single gel slice or from adjacent slices, and the protein was identified in at least two vitreous samples.

**Western blotting.** See **Supplementary Methods** online.

**Retinal vascular permeability.** Male Sprague Dawley ( $n = 278$ ) and Long-Evans ( $n = 12$ ) rats (Taconic Farms) with initial body weights of 250 g were used. Experiments were performed in accordance with guidelines of the Association for Research in Vision and Ophthalmology and with approval from the Animal Care and Use Committee of the Joslin Diabetes Center. Video fluorescein angiography was performed using a scanning laser ophthalmoscope (Rodentock Instrument)<sup>47</sup>. Vitreous fluorophotometry and administration of fluorescein-dextran was performed as previously described<sup>47</sup>. Detailed protocols are described in the **Supplementary Methods**.

**Preparation of lysed RBC and measurement of RVP by Evans blue dye.** To prepare lysed red blood cells (RBC), 3 ml rat blood in 15 ml saline was centrifuged at 500g for 5 min; the plasma and buffy coat were discarded. The RBCs were then washed in 12 ml saline. The packed cells were frozen in liquid nitrogen for 5 min and then allowed to thaw at room temperature  $24^{\circ}\text{C}$ . The

lysed RBCs were centrifuged at 20,800g for 30 min. The supernatant was used for the experiments. The vitreous of rat eyes were injected with BSS, human erythrocyte CA-I (Sigma), lysed RBC or lysed RBC plus acetazolamide in 10  $\mu\text{l}$  final volume. Approximately 21 h later, Evans blue was injected at a dosage of 30 mg per kg (body weight). After the dye had circulated for 3 h, the rats were perfused with saline via the left ventricle. The retinas were harvested, and Evans blue dye was extracted by incubation in 0.3 ml formamide for 20 h at  $60^{\circ}\text{C}$ . The extract was centrifuged, and the absorbance of the filtrate was measured with a spectrophotometer at 620 nm. The concentration of dye in the extracts was calculated from a standard curve.

**Measurements of prekallikrein activation and factor XIIa assay.** Fluorogenic kallikrein substrate (H-D-Val-Leu-Arg-AFC, Calbiochem) was used to quantify kallikrein enzymatic activity. Factor XIIa substrate (H-D-CHT-Gly-L-Arg-pNA diacetate salt, American Diagnostica) was used to quantify FXIIa enzymatic activity produced following prekallikrein activation, kallikrein-mediated FXII activation or FXII autoactivation. Amidolytic activity of FXIIa was measured using 0.5 mM H-D-CHT-Gly-L-Arg-pNA as the substrate in the presence of 20  $\mu\text{M}$  2-tosylamino-4-phenylbutyric acid-(4'-amidinoanilide) hydrochloride (American Diagnostica). Detailed protocols are described in the **Supplementary Methods**.

**High-speed, ultrahigh resolution OCT.** Diabetes was induced in rats by intraperitoneal injection of streptozotocin (55 mg/kg) after overnight fast. Diabetes was confirmed after 24 h by a blood glucose level greater than 13.8 mM. After 2 weeks of diabetes, rats were injected intravitreally with CA-I or BSS and the retinas imaged by OCT after 48 h. The OCT method was as follows: retinal ultrastructure was imaged and quantitatively measured using a high-speed, ultrahigh resolution OCT system with spectral/Fourier domain detection. Using a broadband superluminescent diode light source (Superlum Diodes Limited) with a 155 nm bandwidth, we achieved a 2.8  $\mu\text{m}$  axial resolution in tissue after digital spectral shaping. Measurements of intraretinal layer thicknesses were performed on individual cross-sectional OCT images.

**Evaluation of blood-brain barrier integrity.** CA-I, BSA, C1-INH, lysed RBC or BSS vehicle were perfused into the subdural space 1 mm inferior to the bregma and 1 mm ventral to the skull surface. Approximately 22 h later, Evans blue (30 mg/ml) was injected through a jugular vein catheter at a dosage of 25 mg/kg. After the dye circulated for 2 h, rats were perfused with 50 ml warm saline through the left ventricle. Rats were killed and the concentration of dye in the extracts was calculated from a standard curve of Evans blue in formamide, normalized to the brain weight, and expressed per gram of tissue.

**Statistical analysis.** Kruskal-Wallis analysis of ranks was used to identify differences in protein presence among NDM, noDR and PDR groups. The correlations of CA-I with the presence of other identified vitreous proteins were determined using Spearman correlation coefficients. Other statistical analyses were performed using one-way analysis of variance or paired Student's *t*-test (SigmaStat, Systat Software and Prism, GraphPad Software). Values of  $P < 0.05$  were considered significant.

*Note: Supplementary information is available on the Nature Medicine website.*

## ACKNOWLEDGMENTS

We thank X. Chen and D. Bursell for technical assistance. This work was supported in part by the US National Institutes of Health (grants DK 60165, DK 36836, EY011289 and EY014106), the Juvenile Diabetes Research Foundation (1-2005-1047), the Massachusetts Lions Eye Research Fund, the Adler Foundation and the Air Force Office of Scientific Research Medical Free Electron Laser Program (FA9550-040-1-0046).

## AUTHOR CONTRIBUTIONS

B.-B.G. conducted the proteomic and bioinformatic analysis; performed all western blot and *in vitro* enzymatic analyses, and cerebral vascular permeability experiments; and contributed to manuscript writing. A.C. and S.-E.B. performed retinal permeability analyses, intravitreal injections, and vitreous pH analyses; and assisted in designing the *in vivo* experiments. S.R. assisted with retinal permeability experiments and coordinated vitreous collection. S.J.F. performed proteomic statistical analysis and assisted in editing the manuscript. V.S., M.W. and J.G.F. conducted the OCT measurements, and analyzed and interpreted the

results. R.L.A. and P.G.A. provided vitreous samples and conducted the clinical diagnoses. L.P.A. provided vitreous samples and clinical information, and contributed to manuscript writing. E.P.F. designed the entire study, supervised all components of the study, and wrote the manuscript.

#### COMPETING INTERESTS STATEMENT

The authors declare competing financial interests (see the *Nature Medicine* website for details).

Published online at <http://www.nature.com/naturemedicine/>

Reprints and permissions information is available online at <http://npg.nature.com/reprintsandpermissions>

- Kempner, J.H. *et al.* The prevalence of diabetic retinopathy among adults in the United States. *Arch. Ophthalmol.* **122**, 552–563 (2004).
- Williams, R. *et al.* Epidemiology of diabetic retinopathy and macular oedema: a systematic review. *Eye* **18**, 963–983 (2004).
- The Diabetes Control and Complications Trial Research Group. The effect of intensive treatment of diabetes on the development and progression of long-term complications in insulin-dependent diabetes mellitus. *N. Engl. J. Med.* **329**, 977–986 (1993).
- Stratton, I.M. *et al.* Association of glycaemia with macrovascular and microvascular complications of type 2 diabetes (UKPDS 35): prospective observational study. *Br. Med. J.* **321**, 405–412 (2000).
- UK Prospective Diabetes Study Group. Tight blood pressure control and risk of macrovascular and microvascular complications in type 2 diabetes: UKPDS 38. *Br. Med. J.* **317**, 703–713 (1998).
- Klein, R., Klein, B.E., Moss, S.E. & Cruickshanks, K.J. The Wisconsin epidemiologic study of diabetic retinopathy: XVII. The 14-year incidence and progression of diabetic retinopathy and associated risk factors in type 1 diabetes. *Ophthalmology* **105**, 1801–1815 (1998).
- Ferris, F.L., III, Davis, M.D. & Aiello, L.M. Treatment of diabetic retinopathy. *N. Engl. J. Med.* **341**, 667–678 (1999).
- Klein, R., Klein, B.E., Moss, S.E., Davis, M.D. & DeMets, D.L. The Wisconsin epidemiologic study of diabetic retinopathy. IV. Diabetic macular edema. *Ophthalmology* **91**, 1464–1474 (1984).
- Knudsen, S.T. *et al.* Macular edema reflects generalized vascular hyperpermeability in type 2 diabetic patients with retinopathy. *Diabetes Care* **25**, 2328–2334 (2002).
- Krogsaa, B., Lund-Andersen, H., Mehlsen, J., Sestoft, L. & Larsen, J. The blood-retinal barrier permeability in diabetic patients. *Acta Ophthalmol. (Copenh.)* **59**, 689–694 (1981).
- Plehw, W.E., Sleightholm, M.A. & Kohner, E.M. Does vitreous fluorophotometry reflect severity of early diabetic retinopathy? *Br. J. Ophthalmol.* **73**, 255–260 (1989).
- Lattanzio, R. *et al.* Macular thickness measured by optical coherence tomography (OCT) in diabetic patients. *Eur. J. Ophthalmol.* **12**, 482–487 (2002).
- Aiello, L.P. *et al.* Vascular endothelial growth factor in ocular fluid of patients with diabetic retinopathy and other retinal disorders. *N. Engl. J. Med.* **331**, 1480–1487 (1994).
- Ogata, N., Nishikawa, M., Nishimura, T., Mitsuma, Y. & Matsumura, M. Unbalanced vitreous levels of pigment epithelium-derived factor and vascular endothelial growth factor in diabetic retinopathy. *Am. J. Ophthalmol.* **134**, 348–353 (2002).
- Gragoudas, E.S., Adamis, A.P., Cunningham, E.T., Jr., Feinsod, M. & Guyer, D.R. Pegaptanib for neovascular age-related macular degeneration. *N. Engl. J. Med.* **351**, 2805–2816 (2004).
- Srinivas, S.P., Ong, A., Zhai, C.B. & Bonanno, J.A. Inhibition of carbonic anhydrase activity in cultured bovine corneal endothelial cells by dorzolamide. *Invest. Ophthalmol. Vis. Sci.* **43**, 3273–3278 (2002).
- Wolfensberger, T.J. *et al.* Membrane-bound carbonic anhydrase in human retinal pigment epithelium. *Invest. Ophthalmol. Vis. Sci.* **35**, 3401–3407 (1994).
- Giusti, C., Forte, R., Vingolo, E.M. & Gargiulo, P. Is acetazolamide effective in the treatment of diabetic macular edema? A pilot study. *Int. Ophthalmol.* **24**, 79–88 (2001).
- Miyamoto, K. *et al.* Prevention of leukostasis and vascular leakage in streptozotocin-induced diabetic retinopathy via intercellular adhesion molecule-1 inhibition. *Proc. Natl. Acad. Sci. USA* **96**, 10836–10841 (1999).
- Wojtkowski, M. *et al.* Three dimensional retinal imaging with high-speed, ultrahigh resolution, optical coherence tomography. *Ophthalmology* **112**, 1734–1746 (2005).
- Anderson, N.L. *et al.* The human plasma proteome: a nonredundant list developed by combination of four separate sources. *Mol. Cell. Proteomics* **3**, 311–326 (2004).
- Wistrand, P.J., Schenholm, M. & Lonnerholm, G. Carbonic anhydrase isoenzymes CA I and CA II in the human eye. *Invest. Ophthalmol. Vis. Sci.* **27**, 419–428 (1986).
- Carugati, A., Pappalardo, E., Zingale, L.C. & Cicardi, M. C1-inhibitor deficiency and angioedema. *Mol. Immunol.* **38**, 161–173 (2001).
- Han, E.D., MacFarlane, R.C., Mulligan, A.N., Scafidi, J. & Davis, A.E., III. Increased vascular permeability in C1 inhibitor-deficient mice mediated by the bradykinin type 2 receptor. *J. Clin. Invest.* **109**, 1057–1063 (2002).
- Shariat-Madar, Z., Mahdi, F. & Schmaier, A.H. Identification and characterization of prolylcarboxypeptidase as an endothelial cell prekallikrein activator. *J. Biol. Chem.* **277**, 17962–17969 (2002).
- Houle, S., Molinaro, G., Adam, A. & Marceau, F. Tissue kallikrein actions at the rabbit natural or recombinant kinin B2 receptors. *Hypertension* **41**, 611–617 (2003).
- Veloso, D., Silver, L.D., Hahn, S. & Colman, R.W. A monoclonal anti-human plasma prekallikrein antibody that inhibits activation of prekallikrein by factor XIIa on a surface. *Blood* **70**, 1053–1062 (1987).
- Yang, Z. *et al.* Mutant carbonic anhydrase 4 impairs pH regulation and causes retinal photoreceptor degeneration. *Hum. Mol. Genet.* **14**, 255–265 (2005).
- Xi, G. *et al.* Mechanisms of edema formation after intracerebral hemorrhage: effects of extravasated red blood cells on blood flow and blood-brain barrier integrity. *Stroke* **32**, 2932–2938 (2001).
- Qureshi, A.I. *et al.* Spontaneous intracerebral hemorrhage. *N. Engl. J. Med.* **344**, 1450–1460 (2001).
- Yamane, K. *et al.* Proteome analysis of human vitreous proteins. *Mol. Cell. Proteomics* **2**, 1177–1187 (2003).
- Nakanishi, T., Koyama, R., Ikeda, T. & Shimizu, A. Catalogue of soluble proteins in the human vitreous humor: comparison between diabetic retinopathy and macular hole. *J. Chromatogr. B Analyt. Technol. Biomed. Life Sci.* **776**, 89–100 (2002).
- Ouchi, M., West, K., Crabb, J.W., Kinoshita, S. & Kamei, M. Proteomic analysis of vitreous from diabetic macular edema. *Exp. Eye Res.* **81**, 176–182 (2005).
- Henricsson, M., Sellman, A., Tyrberg, M. & Groop, L. Progression to proliferative retinopathy and macular oedema requiring treatment. Assessment of the alternative classification of the Wisconsin Study. *Acta Ophthalmol. Scand.* **77**, 218–223 (1999).
- Svastova, E. *et al.* Hypoxia activates the capacity of tumor-associated carbonic anhydrase IX to acidify extracellular pH. *FEBS Lett.* **577**, 439–445 (2004).
- Iwaki, T. & Castellino, F.J. Plasma levels of bradykinin are suppressed in factor XII-deficient mice. *Thromb. Haemost.* **95**, 1003–1010 (2006).
- Shariat-Madar, Z., Mahdi, F. & Schmaier, A.H. Recombinant prolylcarboxypeptidase activates plasma prekallikrein. *Blood* **103**, 4554–4561 (2004).
- Joseph, K. & Kaplan, A.P. Formation of bradykinin: a major contributor to the innate inflammatory response. *Adv. Immunol.* **86**, 159–208 (2005).
- Nagelhus, E.A. *et al.* Carbonic anhydrase XIV is enriched in specific membrane domains of retinal pigment epithelium, Muller cells, and astrocytes. *Proc. Natl. Acad. Sci. USA* **102**, 8030–8035 (2005).
- Rassam, S.M., Patel, V. & Kohner, E.M. The effect of acetazolamide on the retinal circulation. *Eye* **7**, 697–702 (1993).
- Vorstrup, S., Henriksen, L. & Paulson, O.B. Effect of acetazolamide on cerebral blood flow and cerebral metabolic rate for oxygen. *J. Clin. Invest.* **74**, 1634–1639 (1984).
- Stefansson, E. *et al.* Optic nerve oxygen tension in pigs and the effect of carbonic anhydrase inhibitors. *Invest. Ophthalmol. Vis. Sci.* **40**, 2756–2761 (1999).
- Weber, A. *et al.* Unexpected nanomolar inhibition of carbonic anhydrase by COX-2-selective celecoxib: new pharmacological opportunities due to related binding site recognition. *J. Med. Chem.* **47**, 550–557 (2004).
- van Doorn, M.B. *et al.* A phase I study of recombinant human C1 inhibitor in asymptomatic patients with hereditary angioedema. *J. Allergy Clin. Immunol.* **116**, 876–883 (2005).
- Kakoki, M., Takahashi, N., Jennette, J.C. & Smithies, O. Diabetic nephropathy is markedly enhanced in mice lacking the bradykinin B2 receptor. *Proc. Natl. Acad. Sci. USA* **101**, 13302–13305 (2004).
- Early Treatment Diabetic Retinopathy Study Research Group. Grading diabetic retinopathy from stereoscopic color fundus photographs—an extension of the modified Airlie House classification. ETDRS report number 10. *Ophthalmology* **98**, 786–806 (1991).
- Aiello, L.P. *et al.* Vascular endothelial growth factor-induced retinal permeability is mediated by protein kinase C *in vivo* and suppressed by an orally effective beta-isoform-selective inhibitor. *Diabetes* **46**, 1473–1480 (1997).